Lithographic lasers with low thermal resistance

A. Demir, G. Zhao and D.G. Deppe

Data are presented demonstrating a low thermal resistance lithographic laser. An 8 μm vertical-cavity surface emitting laser defined using lithography and epitaxial crystal growth provides output power of 14 mW, slope efficiency of 0.88 W/A corresponding to differential quantum efficiency of 70% and power conversion efficiency of 26%. Low thermal resistance, even without heatsinking, results in high output power densities owing to better heat spreading through the epitaxial structure for small lasers.

Introduction: Oxide-confined edge emitting [1–3] and vertical-cavity surface emitting lasers (VCSELs) [4, 5] fabricated using conversion of a buried AlGaAs layer to native oxide of Al_xO_y by selective oxidation have been intensely studied [6, 7]. The oxide-confined quantum-dot edge emitting laser was shown to reach low threshold current densities [3]. The improvements of VCSEL performance are due to simultaneous mode- and current-confinement using the oxide-aperture. The low threshold and low power consumption have produced high-speed modulation and high-efficiency VCSELs [5, 8]. However, the oxide-aperture creates stress because of the difference in the thermal expansion coefficient between the oxide and semiconductor and degrades the reliability of the VCSELs, especially for small apertures, and can be difficult to control for small sizes. The thermal conductivity is also degraded, since the Al_xO_y has a thermal conductivity of 0.7 W/m K while GaAs and AlAs have thermal conductivity of ~50 W/m K [9]. Heat spreading can therefore limit the laser diode power and modulation bandwidth. Reducing the thermal resistance of oxide-confined VCSELs by applying effective heatsinking methods has been demonstrated to increase the device performance by increasing the modulation bandwidth and output power [10].

In this Letter, we demonstrate lithographically-defined laser diodes in which the transverse mode and cavity are defined using only lithography and epitaxial crystal growth. We also show that eliminating the oxide aperture reduces the thermal resistance, with increased power density found in smaller lasers. A low thermal resistance can increase the output power saturation before thermal rollover. When it is combined with better mode matching to gain for smaller devices, high output power densities are possible from small devices. Lithographic definition gives the ability to reach small sizes that are difficult to achieve reproducibly for oxide-aperture lasers. The demonstration of lithographic laser diodes with good scaling properties could therefore be an important step towards producing ultra-small-size laser diodes with high output power density, high manufacturability and high reliability.

Device structure: The devices are grown using solid source molecular beam epitaxy and they are defined lithographically as described in [11]. The VCSEL consists of 21 *n*-type AlAs/GaAs quarter-wave bottom mirror pairs with a $Al_{0.1}Ga_{0.9}As$ one-wavelength cavity spacer and three InGaAs/GaAs quantum wells placed at the centre of the cavity and completed with a *p*-type $Al_{0.7}Ga_{0.3}As$/GaAs mirror stack of 20 pairs. Following the growth, substrate and episide metal contacts are formed and alloyed.

Results: The devices are isolated and tested on a wafer placed on a probe stage without use of additional mounting or heatsinking. Fig. 1 shows the light output against current and the lasing spectrum at 1 mA for an 8 μm-diameter VCSEL. The device has a sub-milliampere threshold current of 710 μA and threshold voltage of 1.55 V. The slope efficiency of the device is 0.88 W/A, corresponding to 70% differential quantum efficiency, which is comparable to the best results achieved by well-developed oxide-confined VCSELs [5]. The maximum power conversion efficiency of 26% is reached at four times the threshold with output power of 1.7 mW. The low threshold and linear trend of output power with injected current indicate stable operation of the laser.

Emission spectra of the laser are plotted in Fig. 2 for sub-threshold (0.5 mA) and above threshold currents including spectra at a very high current level of 18 mA. Several modes are clearly observed at the sub-threshold current of 0.5 mA and only the fundamental mode of the longest wavelength shows lasing at above a threshold current of 1 mA. At higher injection, higher-order transverse modes show up owing to the large size of the confinement region, and they show lasing initially at the longest wavelength. The thermal resistance can be extracted from the shift to longer wavelengths with increasing current and is smaller compared to oxide-aperture VCSELs of the same size.

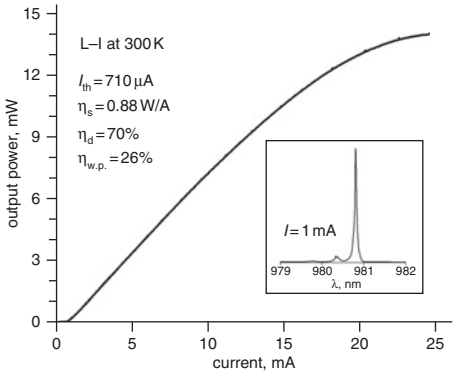

Fig. 1 *Output power against current characteristics of 8 μm-diameter VCSEL*

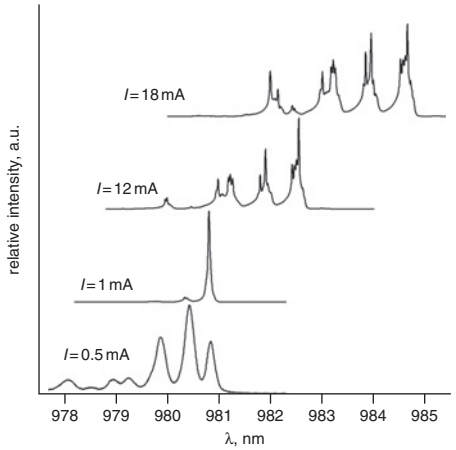

Fig. 2 *Emission spectra of 8 μm-diameter device for various current levels below (0.5 mA) and above threshold (1, 12 and 18 mA)*

The thermal resistance of the lithographic laser diodes was found for different laser diode sizes using the variation of the emission wavelength with the change in dissipated power. Using 0.07 nm/K for the wavelength shift with temperature [5, 10], Fig. 3 demonstrates the thermal resistances of the VCSELs measured for device sizes ranging from 3 to 20 μm in diameter. Fig. 3 also compares the results of the lithographic lasers to the data in the literature obtained for epi-side-up mounting of oxide-confined VCSELs by various groups [5, 10, 12, 13]. The thermal resistance of the lithographic lasers is consistently reduced to about 60% over the best reported results we have found for oxide-confined VCSELs that use copper plating on the epitaxial side [10], and to about 30% over epi-up mounted VCSELs without copper plating.

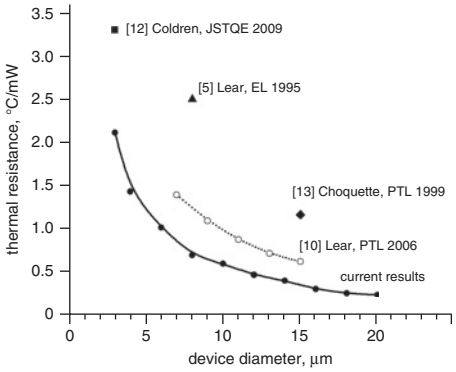

Fig. 3 *Thermal resistance against device diameter of lithographic VCSEL and its comparison to oxide-confined VCSELs*

As the lithographic laser diode size is reduced the heat spreading becomes more three-dimensional owing to the absence of the oxide. This enables the smaller sizes to be operated at high current density and high power density. The absence of oxide strain results in no measurable degradation even for the smallest device sizes made so far (3 μm diameter) for operation of tens of hours in the laboratory. This is in contrast to our experience on small oxide VCSELs, which often show degradation owing to oxide strain. The maximum power density before thermal limiting for the different device sizes is shown in Fig. 4. The smallest laser sizes show the largest maximum power and current densities before the thermal limit, with the 3 μm size capable of operating at ~100 kA/cm^2 and more than 55 kW/cm^2 before heating saturates the output power.

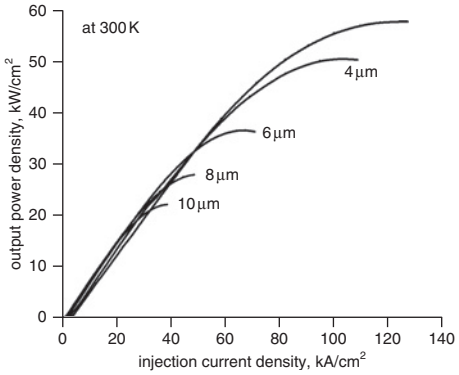

Fig. 4 *Output power density against injection current density, showing that output power density is highest for smallest device size tested*

The thresholds and slope efficiencies of the different device sizes show that the currents are well confined to the mesas. The thresholds and slope efficiencies are 0.26 mA and 0.76 W/A for the 3 μm device, 0.34 mA and 0.79 W/A for the 4 μm device, 0.48 mA and 0.81 W/A for the 6 μm device, and 0.71 mA and 0.88 W/A for the 8 μm device. The data demonstrate that the slope efficiencies are high and almost unchanged for different sizes, while the thresholds scale with the device sizes owing to current confinement to the lithographically defined mesas. In addition, the output power density increases for smaller sizes and this again shows that the currents are confined to the mesas.

Small-sized VCSELs generally can be made to operate at high modulation rates [12], and are also important for low power sensors that require singlemode operation and singlemode arrays for increased power and brightness. The lithographic approach can have advantages in these applications because of its increased uniformity, reduced internal strain, and reduced thermal resistance for either epi-side-up or epi-side-down mounting.

Conclusion: We have demonstrated lithographic lasers based on VCSELs that show good scaling properties and reduced thermal resistance as compared to oxide VCSELs. The lithographic laser solves problems of oxide-confined VCSELs of strain and size control, enabling small VCSEL sizes to be realised with the potential for improved manufacturability. The epitaxial approach can also extend the VCSEL technology to high reliability and fully planar VCSELs and dense VCSEL arrays, since etch requirements are minimal. The lithographic laser characteristics show increased output power density with reduced device size owing to increased three-dimensional heat flow.

4 June 2010
doi: 10.1049/el.2010.8532

A. Demir, G. Zhao and D.G. Deppe (*CREOL, College of Optics & Photonics, University of Central Florida, Orlando, FL 32618, USA*)

E-mail: ademir@creol.ucf.edu

References

1 Maranowski, S.A., Sugg, A.R., Chen, E.I., and Holonyak, N. Jr.: 'Native oxide top- and bottom-confined narrow stripe p-n AlGaAs–GaAs–In-GaAs quantum well heterostructure laser', *Appl. Phys. Lett.*, 1993, **63**, pp. 1660–1662
2 Cheng, Y., Dapkus, P.D., MacDougal, M.H., and Yang, G.M.: 'Lasing characteristics of high performance narrow-stripe InGaAs–GaAs quantum-well lasers confined by AlAs native oxide', *IEEE Photonics Technol. Lett.*, 1996, **8**, pp. 176–178
3 Park, G., Shchekin, O., Huffaker, D., and Deppe, D.G.: 'Low-threshold oxide-confined 1.3 μm quantum-dot laser', *IEEE Photonics Technol. Lett.*, 2000, **13**, pp. 230–232
4 Huffaker, D.L., Deppe, D.G., Kumar, K., and Rogers, T.J.: 'Native-oxide defined ring contact for low threshold vertical-cavity lasers', *Appl. Phys. Lett.*, 1994, **65**, pp. 97–99
5 Lear, K.L., Choquette, K.D., Schneider, R.P., Kilcoyne, S.P., and Geib, K.M.: 'Selectively oxidised vertical cavity surface emitting lasers with 50% power conversion efficiency', *Electron. Lett.*, 1995, **31**, pp. 208–209
6 Dallesasse, J.M., Holonyak, N., Sugg, A.R., Richard, T.A., and El-Zein, N.: 'Hydrolyzation oxidation of AlxGa1 − xAs-AlAs-GaAs quantum well heterostructures and superlattices', *Appl. Phys. Lett.*, 1990, **57**, pp. 2844–2846
7 Sugg, A.R., Chen, E.I., Richard, T.A., Holonyak, N., and Hsieh, K.C.: 'Native oxide-embedded AlyGa1 − yAs-GaAs-InxGa1 − xAs quantum well heterostructure lasers', *Appl. Phys. Lett.*, 1993, **62**, pp. 1259–1261
8 Jager, R., Grabherr, M., Jung, C., Michalzik, R., Reiner, G., Weigl, B., and Ebeling, K.J.: '57% wallplug efficiency oxide-confined 850 nm wavelength GaAs VCSELs', *Electron. Lett.*, 1997, **33**, pp. 330–331
9 Lee, H.K., Song, Y.M., Lee, Y.T., and Yu, J.S.: 'Thermal analysis of asymmetric intracavity-contacted oxide-aperture VCSELs for efficient heat dissipation', *Solid-State Electron.*, 2009, **53**, pp. 1086–1091
10 Al-Omari, A.N., Carey, G.P., Hallstein, S., Watson, J.P., Dang, G., and Lear, K.L.: 'Low thermal resistance high-speed top-emitting 980-nm VCSELs', *IEEE Photonics Technol. Lett.*, 2006, **18**, pp. 1225–1227
11 Ahn, J., Lu, D., and Deppe, D.G.: 'All-epitaxial, lithographically defined, current and mode-confined vertical-cavity surface-emitting laser based on selective interfacial fermi-level pinning', *Appl. Phys. Lett.*, 2005, **86**, p. 21106
12 Chang, Y.C., and Coldren, L.A.: 'Efficient, high-data-rate, tapered oxide-aperture vertical-cavity surface-emitting lasers', *IEEE J. Sel. Top. Quantum Electron.*, 2009, **15**, pp. 1–12
13 Pu, R., Wilmsen, C.W., Geib, K.M., and Choquette, K.D.: 'Thermal resistance of VCSEL's bonded to integrated circuits', *IEEE Photonics Technol. Lett.*, 1999, **11**, pp. 1554–1556